Technical Note

1966-41

M. L. Burrows

The Quality
of the
Lincoln Calibration Sphere

22 August 1966

AD0638442

MASSACHUSETTS INSTITUTE OF TECHNOLOGY

LINCOLN LABORATORY

THE QUALITY
OF THE LINCOLN CALIBRATION SPHERE

M. L. BURROWS

Group 61

TECHNICAL NOTE 1966-41

22 AUGUST 1966

LEXINGTON   MASSACHUSETTS

The Quality of the Lincoln Calibration Sphere

ABSTRACT

Due to the relatively high background noise level of the radar range used to measure the Lincoln Calibration Sphere (LCS) before launch, the upper-bound estimates of the backscattering cross section variation made at the time included a large contribution generated by the range itself. By comparing the range measurements and the mechanical measurements made on the LCS with measurements made on three other similarly constructed spheres, a refined estimate of the quality of the LCS is made. The comparison makes use of more precise range and mechanical measurements made on the other three spheres and of an application of perturbation theory to compute the variation of cross section from the mechanical measurements. The unexpectedly large signal scattered by the equatorial joint is an unwelcome addition to the backscattered field and is discussed in some detail.

It is concluded that, at all frequencies below about 25 GHz, the r.m.s. deviation in backscattering cross section is not greater than 0.15 db, and that the average backscattering cross section differs from that of a perfect sphere of radius 0.56469 m by an amount which is small compared with the r.m.s. deviation.

The Quality of the Lincoln Calibration Sphere

I. INTRODUCTION

The Lincoln Calibration Sphere (LCS) is a polished aluminum sphere having a nominal geometric cross-sectional area of one square meter. On May 6, 1965, it was launched into a nearly circular, 1500-nautical-mile orbit to serve as a radar calibration target.[1] The backscattering cross section was measured as a function of angle of rotation about three separate axes before launch on a radar cross section range. The measurements were carried out at frequencies in the microwave bands L, S, C, X and K.

It was observed at the time that the variation in cross section indicated on the range record contained a large contribution from the background noise of the range. This observation was based on the fact that there was no recognizable similarity between two successive range records when the only physical difference was that the second record was taken with the sphere displaced by 90°, from its original position on the column, about the column axis. The observation was supported by estimates of the cross section variation based on mechanical measurements of the sphere. These estimates were considerably lower than the indicated variation, but the mechanical measurements made were not sufficiently detailed to enable a direct computation of the cross section variation to be carried out.

However, a number of spheres were produced during the LCS program.

Two were intended for orbiting and others were made as insurance against accidental damage to the flight spheres during manufacture, shipping and measurement. The spheres were all assembled and machined in the same way. Thus, the possibility arose of making more careful measurements on the remaining spheres, to obtain an accurate measure of their quality as radar calibration targets, and then comparing the LCS measurements with these to obtain a better estimate of its quality.

At an early stage in the comparison program it became clear that the surface quality of the LCS is about as good as or better than that of the other spheres. Since the radar cross section variation of these other spheres attributable to surface deviations is, for example, of the order of 0.05 db r.m.s. at X-band, the conclusion was that the same would be true for the LCS. The range measurements made on the LCS at X-band indicated a cross section variation of 0.22 db, so that the revised estimate is a considerable improvement.

Unfortunately, another source of cross section variation was disclosed by the comparison program. Each sphere was constructed by spinning from aluminum sheet two hemispherical shells which, after trimming, were mated by fastening them to a common internal circumferential hoop with countersunk aluminum screws. For location purposes, there was a central tongue one quarter of an inch wide running right around the hoop. The edges of each hemisphere were butted against the tongue during screwing. The whole

2

assembly was machined to size on a vertical boring mill and the surface finished by hand polishing. It was found that unless great care was taken to butt the edges of each hemisphere tightly against the tongue, the slight gaps remaining could cause relatively large variations in radar cross section.

Figure 1 shows two consecutive radar range records obtained at X-band on one of the spheres (the "C" sphere) using horizontal polarization with the sphere rotating about a vertical axis lying in the plane of the circumferential joint. The physical difference between the two measurements was that the lower record was taken with aluminized adhesive tape covering the two butt-lines of the joint. In this case, the records show the unclosed butt joints to cause a peak-to-peak variation in cross section of about 0.7 db. On examining the joint of this sphere, it was found that one hemisphere was tightly butted against the tongue but that a non-uniform gap of about 0.01 inch or less existed along the other edge of the tongue.

The possibility of such a large gap effect was not considered before the LCS launch, and so no measurements of the width of the gaps on the LCS were made. Thus although a good estimate can be obtained for the surface contribution to the variation in cross section, it is more difficult to comment on the variation contributed by the joint.

However, one redeeming feature of the presence of a signal scattered by the joint is that it displays a very clear signature on the radar range record, as shown in Fig. 1. The oscillations are very regular and their period at any

3

particular point on the record can accurately be predicted theoretically. Thus, since the form of the joint signature is known in advance and since it is also very regular, the presence of a relatively small joint signal in the noise-like signals from other sources should be detectable visually. On this basis, the range records obtained with the LCS have been inspected, and where no joint signal appears to be present, an estimate is made of the maximum amplitude that such a signal could have without being visible on the record. This estimate is then used as an upper bound on the effect of the joint.

Of the total of five spheres manufactured in the manner described, one was distinctly atypical. A machining error caused it to have excessive dimensional variations in addition to rendering it mechanically unsound. One of the other four is the LCS and the remaining three were used as a basis for the comparison program. To conform to the designation used in the LCS program, these will be referred to as the C, F and G spheres.

It will be assumed throughout that a linear relationship exists between the backscattering cross section measured in dbm and the backscattering cross section in square meters. Although the relationship between the two is actually logarithmic, all values of cross section encountered lie between ± 1 dbm over which range the linear law is very accurate.

II. SURFACE QUALITY

The C sphere was manufactured at the same time as the LCS and was subjected to the same mechanical and range measurements. One special feature

4

of the C sphere was that a crescent shaped "flat" was present on its surface at a position roughly 34° away from one pole of the sphere and extending about three quarters of the way round at this latitude. Some misalignment during the machining operation caused the spherical surface traversed by the tool to pass outside the material of the sphere in this region and therefore leave it unmachined. The maximum width of the flat was about 7° and its maximum depth was about 0.016 inch. The LCS and the F and G spheres had no imperfections of this type.

Since the spheres were machined on a vertical boring mill, they are essentially bodies of revolution. Surface deviations are therefore extremely small along lines of latitude and the quality of the spheres depends solely on the deviations in the longitudinal direction.

Table I summarizes the original range measurements made on the LCS and C sphere, with the sphere rotating about a vertical axis lying in the equatorial plane. That is, the cross section variation was measured as a function of polar angle. The figures given are the r.m.s. deviations of a full 360° record taken at the frequencies and polarizations indicated.

If the cross section variation of the spheres was not completely swamped by the range background noise, then the table indicates that the LCS is more uniform in cross section than the C sphere except at the lower frequencies. However, at L-band two consecutive range records taken under identical circumstances were apparently completely uncorrelated, and this was true for

5

TABLE I

Range Measurements on LCS and C Sphere

Frequency		Polarization	r. m. s. Deviation dbm	
GHz	Band		LCS	C Sphere
1.335	L	hh	0.288	0.168
3.3	S	hh	0.130	0.123
5.6	C	hh	0.160	0.160
8.5	X	hh	0.220	0.449
8.5	X	vv	0.170	0.261
24.0	K	hh	0.321	0.434

every such pair of records taken. Thus, the L-band entries in the table give

no information about the spheres.

A comparison of the significant mechanical measurements made on all

four spheres is given in Table II. The diameter measurements were made at

18 equally spaced points along a line of longitude. The template measurements

were made with a template in the form of a 40° arc of radius effectively equal

to the mean sphere radius. The figures given are the r. m. s. deviations of

the two central template measurements taken with the template lying along

lines of longitude and not bridging either the poles or the equator. Only the

two central readings are used, of the four uniformly spaced readings actually

taken at each position of the template, because the surface nearer the template

leg is more closely correlated with the surface at the leg, which makes the

two outer readings less easy to interpret.

TABLE II

Mechanical Measurements

Sphere	Diameter Measurements		Template Measurements	
	No. of Points	r.m.s. dev., inch	No. of Points	r.m.s. dev., inch
LCS	18	0.0062	80	0.00177
C	18*	0.0146	60*	0.00165
F	18	0.0119	48	0.00241
G	18	0.0054	80	0.00224

* Points in the flat crescent excluded.

By excluding those template readings made with the template bridging poles or the equator, it is possible to regard the r.m.s. deviation of the template readings as a measure of the quality of the arc forming ability of the machining operation and the diameter measurements as a measure of the accuracy with which these arcs were aligned by the setting up operation. If the setting up operation is not done accurately, it is possible to obtain a sphere with, for example, a dimple at each pole and a cusp around the equator, even though each 90° arc of the polar profile is truely circular. A complete point-by-point polar profile measurement of the C sphere showed that it is of this form, and this is indicated by the large diameter variation given for this sphere in Table II.

7

A comparison of the measurements given in the table shows that the surface quality of the LCS is about as good as or better than that of the other three spheres.

No standard radar cross section range has a sufficiently low noise level to give directly an unambiguous measurement of the quality of these precise spheres. To obtain such a measurement, therefore, detailed mechanical measurements were made on the three remaining spheres after the launch of the LCS and these were used to compute their cross section variation. The computations were checked by comparing clearly marked features in the computed cross section variation with measurements made on a range having a lower noise level than that of the one originally used.

The computations are an application of classical boundary perturbation theory and take advantage of the assumption that the spheres are essentially bodies of revolution.[2] If this assumption is true, then the shape of the spheres is defined by the shape of a single line of longitude.

Figure 2 shows a plot of three profile measurements made on the G sphere. These were made by rotating the sphere on a turntable and measuring the surface deviations at one degree intervals with a dial gauge. The difference between the two latitude profiles and the polar profile is very marked. The equatorial profile (0° latitude) shows greater variation than the 45° profile because the screwed joint is at the equator and also the equator is at the junction of the two arcs defined by the machining operation. The 45° profile

is therefore more typical of the surface variation along lines of latitude, and by comparison with the polar profile, it substantiates the assumption that the sphere is a body of revolution.

A complete 360° polar profile measurement contains two essentially similar half-profiles each of which can be used as the definition of the shape of the sphere. The radar cross section of the sphere was computed for the body defined by each half profile and then this was repeated using a second complete 360° polar profile taken along the lines of longitude displaced by 90° from the first. Thus, for each sphere, a total of four separate half profiles were obtained from which four separate computations of the radar cross section variation were made.

The results for the G sphere over the frequency range 1 − 30 GHz are shown in Fig. 3 as the four solid curves joining sets of four computed points. The closeness of the four lines shows that the high degree of axial symmetry in the mechanical measurements is accompanied by a correspondingly high degree of axial symmetry in this aspect of the scattering properties. A further demonstration of the effect of neglecting the azimuthal surface variation is given by the dashed curves, which were obtained by using the same computer program operating on the 45° latitude profile measurements. These dashed curves do not, of course, represent any real cross section statistics. Each is the cross section variation of a body of revolution whose polar half profile is the same curve as one half of the equatorial profile of the G sphere.

The computations were actually carried out for both circular and linear polarization, but the difference between them was so small in every case that they are indistinguishable when plotted in the manner of Fig. 3. In computing the r. m. s. deviation of the cross section, the averaging was carried out over all aspect angles contained in the 4π steradian solid angle "aspect space" and, in the case of linear polarization, over all directions of polarization as well. However, the surface quality of the spheres is such that the cross section variation due to this source is essentially independent of polarization. (This is not the case for the joint contribution to the variation, to be discussed later.)

The three isolated points at 9.4 MHz in Fig. 3 were obtained from a radar range measurement of the sphere. Each of the upper two is the r. m. s. deviation of a single 360° polar profile measurement of the radar cross section, the difference being the direction of polarization used. The lower point was obtained by first averaging eight half profiles taken around the poles and then computing the r. m. s. deviation of this mean half profile. This was done to reduce the effect of the background noise of the range. The attempt appears to have been successful, for the agreement between this point and the computed curves is very good.

The possibility of a large joint contribution was known before the F and G spheres were made, and so careful attention was given to ensure that the hemisphere edges were butted tightly against the hoop tongue. In addition a

10

loaded epoxy filler was applied during mating to fill what gap might be present. Thus both the F and G spheres were free of any visible joint contribution to their cross section variation when measured at X-band, and the comparison of the measured radar quality with that computed from the surface measurements is not complicated by unknown joint effects.

Figures 4 and 5 display the results for the F and C spheres corresponding to those for the G sphere already given in Fig. 3. No computations based on a 45° latitude profile are presented for these spheres, and, since the C sphere had a large joint contribution, no computation of the variation of the mean of 8 half-profile range measurements was made.

The F sphere results show a reasonable agreement between the computed variation and the variation obtained from the range records. The spread between the four computed curves, however, is larger for this sphere than for the G sphere, but it is still small enough to enable any one of them to be used to characterize the radar quality of this sphere.

The C sphere results (Fig. 5), are markedly different, due to the presence of the flat crescent on the C sphere. Of the four half-profile measurements made, one was made along a line of longitude which did not pass through the flat and the other three were taken along lines which passed through it at different places. Thus, the four computations of the variation in radar cross section are based upon four bodies of revolution which are essentially similar and closely spherical but differ in the width and depth of a flat zone. The

curves show, as would be expected, a radar cross section variation which in-creases with the size of the flat zone. The bottom curve is therefore a good estimate of the quality of the C sphere were the flat crescent to be filled in, since this is the one based upon the half profile taken along a line of longitude not passing through the flat crescent.

As an indication of the accuracy with which it was possible to calculate the point-to-point variation in cross section (rather than the averaged varia-tion plotted in Figs. 3, 4 and 5), the calculated cross section of the C sphere at 9.3 GHz as a function of latitude along a line of longitude is plotted in Fig. 6 in the vicinity of the flat crescent. The particular half profile used for the computations is plotted in part and is that for which the flat crescent depression was most marked. Also shown is the cross section variation at 9.3 GHz taken from the radar range record for the same line of longitude. The agree-ment between the computed and the measured cross section is fairly good when it is considered that the background level of the range varied between -30 and -40 dbm and so could account for discrepancies as large as ± 0.15 db. The fact that the computed variation of cross section is larger than that mea-sured, as the line of sight passes through the flat crescent, is probably due to the fact that the computations were made on the assumption that the depression shown in the profile measurement existed uniformly around the sphere at that latitude, thus forming a complete flat zone rather than a flat crescent. Thus, the sphere used for the computations was "worse" than the sphere actually

12

measured on the range.

A comparison of the computed curves for the three spheres as plotted in Figs. 3, 4 and 5 shows that all the F and G curves and the "C-without-flat" curve can be contained in a relatively narrow band. Since the experimental results have corroborated the computed curves, one can conclude that these three spheres are roughly equal in radar quality (excluding the joint contribution). But the LCS was made in exactly the same way as the other three spheres, and a comparison of mechanical measurements shows its surface quality to be as good as or better than that of the others, so the radar quality of the three must be representative of the radar quality of the LCS.

In Fig. 7, the band containing all the F and G curves and the "C-without-flat" curve is illustrated, together with the original range measurements on the LCS obtained from Table I. The upper boundary of the band will be taken as the revised estimate of the surface contribution to the cross section variation of the LCS. It is clear that the surface quality of the LCS is considerably better than was indicated by the original range measurements.

III. SCATTERING FROM THE JOINT

The radar signature of the signal backscattered by the joint has been studied theoretically and the results are presented as an Appendix. It is shown there, for the configuration illustrated in Fig. 8, that the change in back-scattering cross section due to the presence of a uniform slot around the equator and measured with a radar polarized in the x direction both on trans-

mission and reception, is given by

$$\delta\sigma_x(\theta_o) = \beta \, \frac{\cos\,(2ka\,\sin\theta_o + \psi_o)}{\sqrt{\sin\theta_o}} \tag{1}$$

for θ_o not close to zero, and

$$|\delta\sigma_x(0)| \leq \frac{\beta}{2}\sqrt{\pi ka} \quad , \tag{2}$$

where a is the sphere radius and $k = 2\pi/\lambda$. The unknown real constants β and ψ_o, and the inequality in (2) are necessary because the complex slot impedance is unknown.

The corresponding quantity $\delta\sigma_y(\theta_o)$ for a y-polarized measurement is shown to be small compared with $\delta\sigma_x(\theta_o)$ for θ_o not close to zero and to be equal to $\delta\sigma_x(0)$ at the point $\theta_o = 0$.

In Fig. 9, sections of two range records obtained at 9.3 GHz during measurements of the C sphere are plotted. The uppermost curve was obtained with the radar polarized to measure $\delta\sigma_x(\theta_o)$ and the bottom curve with it measuring $\delta\sigma_y(\theta_o)$. The middle curve is a plot of $\delta\sigma_x(\theta_o)$ as given by (1) and (2) with a particular choice of β and ψ_o and the value of ka (110) appropriate for this frequency and the radius of sphere C. It is clear that the theoretical model accurately predicts the instantaneous period of the oscillations due to the joint but, since the imperfections of the actual joint are not uniform around the equator, the envelope of the oscillations does not match well. The

14

absence of a marked peak in the measured oscillations for θ_o close to zero can be attributed to this, and also possibly to the great directivity of the peak, which demands a very accurate alignment of the sphere on the column if it is to be observed. The measured curve of $\delta\sigma_y(\theta_o)$ confirms the theoretical prediction that essentially no joint-scattered signal should be observed for this polarization.

In the Appendix [equations (A. 14) and (A. 15)] it is shown that the variance of the cross section variation due to the joint is given by $3\pi\beta^2/32$ for linear polarization and $\pi\beta^2/16$ for circular polarization, when the averaging is carried out over all aspects and, in the former case, polarizations.

Thus by inspecting the $\delta\sigma_x(\theta_o)$ radar range measurements of the LCS for the presence of the characteristic joint signature and estimating β, the peak amplitude of the oscillations when θ_o is not close to zero, the statistical contribution of the joint scattered signal to the total cross section variation can be evaluated. The results are shown in Table III.

The numbers in the column labelled "r. m. s. deviation" are taken from Table I and are included as a measure of the amplitude of the "noise" in which the joint signal was sought. Only at two frequencies was there an unambiguous joint signal present, where it persisted very regularly over more than half of each 360° record. (This was not noticed at the time the measurements were made, because the form of the joint signature was unknown and the regular ripple on the record was attributed to varying multipath effects

15

TABLE III

Results of Inspection for a Joint Signal in the LCS
Range Records

Frequency		r. m. s. deviation (dbm)	β (dbm)	Visually Present?	Estimated Variance (dbm^2)
Band	GHz				
L	1.335	0.288	< 0.2	No	0.012
S	3.3	0.130	$\lesssim$ 0.1	Possibly	0.003
C	5.6	0.160	0.2	Yes	0.012
X	8.5	0.220	0.2	Yes	0.012
K	24.0	0.321	< 0.2	No	0.012

generated by the rotation and by the wind-induced sway of the sphere and column.) At those frequencies where the joint signal was not visually apparent, an estimate was made of the upper bound on β for it not to be seen. The last column is the variance of the cross section, computed using the linear polarization expression $3\pi\beta^2/32$ [equation (A.14) in the Appendix] and the estimate of β, or its upper bound, appearing in the adjoining column. The corresponding variance for circular polarization is smaller by the factor 2/3, but since upper bounds are the quantities of interest, these figures are not listed.

The values of β listed in Table III appear to indicate a joint signal which is maximum in the vicinity of C and X-bands and decreasing as the frequency is reduced below or increased above this region of the spectrum. This

behavior is in accord with a more detailed examination of the scattering pro-
perties of a slot. At sufficiently high frequencies the displacement current
across the edges of the slot is large enough to carry the conduction current
across the slot essentially without impediment. At very low frequencies, on
the other hand, the conduction currents can flow from one edge down into the
slot and eventually reach the other edge by a conductive path which is small
compared with a wavelength. Since the depth of the slots in the LCS is about
1/8 inch, this condition would be expected to be reached in the vicinity of the
L and S frequency bands.

The estimated upper bounds on the cross section variance listed in
Table III are all equal to 0.012 dbm^2 except for the S-band bound, which is
smaller. To facilitate the presentation of the final results it is more conve-
nient to set the S-band bound at 0.012 dbm^2, too.

IV. THE MEAN CROSS SECTION

The average diameter of the LCS, obtained by averaging the 18 polar
profile diameter measurements with respect to the weight function $\sin\theta$, was
found to be 44.464 inch. Thus the mean radius is 0.56469 m. The nominal
radius is 0.56419 m, since for this the geometrical cross-sectional area is
1 m^2.

First order perturbation theory[2] has been used in Section II to compute
the variations in backscattering cross section plotted in the various graphs
referred to in that section, apparently with good results. This means that no

17

great error has been incurred by neglecting the higher order perturbation contributions. But in the first order approximation, the mean cross section is the cross section of the mean sphere. Therefore, one concludes that the mean backscattering cross section of the LCS is equal to that of a sphere of radius 0.56469 m to within an error that must be small compared with the r.m.s. deviation of the backscattering cross section, for which an upper bound estimate is given in Fig. 10.

V. CONCLUSION

If the reasonable assumption is made that the signal scattered by the joint and the signal scattered by the surface perturbations are statistically independent, then the variance of the total cross section is equal to the sum of the variances of the cross section deviations due to each separately. From the upper bound estimates of these quantities obtained in Sections II and III, the resultant upper bound on the r.m.s. deviation of the total backscattering cross section is found to be as shown in Fig. 10. The averaging is carried out over all aspects and all directions of linear polarization.

The upper bound shown is probably excessively high at the lower end of the frequency range plotted, but no information is available on which to base a better estimate.

Since the signal scattered by the joint is sensitive to the direction of polarization, the bound for circular polarization is slightly lower than that shown.

The mean backscattering cross section of the LCS is equal to that of a sphere of radius 0.56469 m to within an error which is small compared with the r.m.s. deviation of the cross section. The backscattering cross section of such a sphere as a function of frequency can be obtained, for example, from the tabulated computations of Rheinstein.[4]

ACKNOWLEDGMENT

19

APPENDIX

Since a butted joint on a conducting surface is a barrier to the surface current flowing in a direction perpendicular to the line of the joint, it is conjectured that the joint behaves like a slot antenna with a voltage across it proportional to the transverse current density that would exist at the position of the joint were the joint not there. The factor of proportionality can be interpreted in terms of the impedance of the slot, but the radar signature of the slot can be obtained to within this factor without evaluating the impedance.

Over the illuminated side of the LCS and at the frequencies of interest, the surface current $\overline{K}$ is given closely by the tangent plane approximation

$$\overline{K} = 2\hat{n} \times \overline{H}$$

where $\hat{n}$ is the unit normal to the surface and $\overline{H}$ is the incident magnetic field strength. Accordingly, the voltage $\overline{V}$ across the slot is given by

$$\overline{V} = \alpha\hat{\ell} \times \hat{n}\,\overline{H} \cdot \hat{\ell} \quad ,$$

where α is the factor of proportionality and $\hat{\ell}$ is a unit vector directed along the slot. But a slot antenna in the surface is equivalent to a magnetic line current $\overline{I}_m$ in the surface given by $\overline{I}_m = \hat{n} \times \overline{V}$, so that

$$\overline{I}_m = \alpha\hat{\ell}\,\overline{H} \cdot \hat{\ell} \quad . \tag{A.1}$$

20

The field $\delta\overline{E}$ radiated by this equivalent slot current is therefore[2]

$$\delta\overline{E}(\overline{r}) = \frac{i}{\omega} \int \overline{\overline{\mathcal{G}}}^{(m)}(\overline{r};\overline{r}') \cdot \overline{I}_m(\overline{r}')\, d\ell \quad , \tag{A.2}$$

where $\overline{\overline{\mathcal{G}}}^{(m)}(\overline{r};\overline{r}')$ is that Green's dyadic for the sphere, giving the electric field at $\overline{r}$ due to a unit magnetic dipole at $\overline{r}'$, and the integration is carried out over the length of the slot.

By reciprocity,[2] $\overline{\overline{\mathcal{G}}}^{(m)}(\overline{r};\overline{r}') = -\,[\overline{\overline{\mathcal{H}}}^{(e)}(\overline{r}';\overline{r})]^T$, where $\overline{\overline{\mathcal{H}}}^{(e)}(\overline{r}';\overline{r})$ is that Green's dyadic giving the magnetic field at $\overline{r}'$ due to a unit electric dipole source at $\overline{r}$ and $[\ \ ]^T$ denotes "transpose of." Therefore, (A.1) and (A.2) can be combined as

$$\delta E(\overline{r}) = \int \alpha \overline{H} \cdot \hat{\ell}\ \ \hat{\ell} \cdot \overline{H}'\, d\ell \quad , \tag{A.3}$$

where δE is a selected vector component of $\delta\overline{E}(\overline{r})$ for r in the far field, $\overline{H}'$ is the magnetic field at the surface of the sphere due to a test incident plane wave polarized in the direction of the selected component and the various proportionality factors have been absorbed by α. Since the impedance of the slot may in general be a function of position along the slot, α is included under the integral sign.

The radar signature of the butt joints on the sphere is computed by assuming that the two joints either side of the hoop tongue, being separated by

only 0.25 inch, can be treated as a single one midway between then, which is at the equator of the sphere. It is also assumed that the slot impedance is essentially uniform so that α can be factored out from the integration in (A.3).

No generality is lost by assuming that the polar axis of the sphere lies in the plane y = 0 of a rectangular coordinate system and is inclined to the z axis by the angle θ_o. The incident plane wave is assumed to be traveling in the negative z direction. This configuration is illustrated in Fig. 8.

For a plane wave polarized in the $\begin{Bmatrix} x \\ y \end{Bmatrix}$ direction, the tangent plane approximations for the components of the magnetic field are proportional to

$$H_\theta = \cos\theta \ e^{-ika\cos\theta} \begin{Bmatrix} -\sin\varphi \\ \cos\varphi \end{Bmatrix}$$

$$H_\varphi = e^{-ika\cos\theta} \begin{Bmatrix} -\cos\varphi \\ -\sin\varphi \end{Bmatrix} \quad ,$$

(A.4)

in a spherical coordinate system with polar axis along the z axis, where a is the sphere radius. If φ_o is the azimuth coordinate in the natural coordinates of the sphere, the component of the magnetic field along the slot is given by

$$\bar{H} \cdot \hat{\ell} = H_\theta \frac{\partial\theta}{\partial\varphi_o} + H_\varphi \sin\theta \frac{\partial\varphi}{\partial\varphi_o} \quad .$$

(A.5)

By taking the polarizations of the incident plane waves (actual and test) each to be either in the x or y directions, it is a simple matter to show from (A.3),

22

(A. 4) and (A. 5), together with the elementary geometrical relationships connecting the two spherical coordinate systems, that

$$
\begin{Bmatrix} \delta E_{xx} \\ \delta E_{yy} \\ \delta E_{xy} \end{Bmatrix} = \alpha \int \begin{Bmatrix} \cos^2 \varphi_o \\ \sin^2 \varphi_o \cos^2 \theta_o \\ \sin \varphi_o \cos \varphi_o \cos \theta_o \end{Bmatrix} \exp(i2ka \cos \varphi_o \sin \theta_o) \, d\varphi_o \quad ,
$$

(A. 6)

where δE_{ij} is the i - directed component of the field radiated by the slot when the incident field is polarized in the j direction and $\delta E_{ij} = \delta E_{ji}$. The integration is to be carried out over the illuminated semicircle of the slot.

Since, in the case of δE_{xy}, the integrand is an odd function, $\delta E_{xy} \equiv 0$. The other two joint fields can be evaluated by the method of stationary phase, provided θ_o is bounded away from zero. The stationary phase point is at $\varphi_o = \pi$, so that

$$
\delta E_{xx} = \alpha \sqrt{\frac{i\pi}{ka \sin \theta_o}} \, e^{-i2ka \sin \theta_o} \quad , \quad (\theta_o \neq 0)
$$

(A. 7)

and, since $\sin^2 \varphi_o$ is $O(\varphi_o^2)$ at the stationary phase point,

$$
\delta E_{yy} = \alpha O \left\{ (ka)^{-3/2} \right\} \quad , \quad (\theta_o \neq 0) \quad .
$$

(A. 8)

23

Thus δE_{xx} is the only significant member of the set defined by (A.6) when θ_o is bounded away from zero.

When θ_o is in the vicinity of zero, a different situation obtains, for the substitution $\theta_o = 0$ into (A.6) leads to $\delta E_{xx} = \delta E_{yy}$. It is not permissible to evaluate (A.6) for $\theta_o = 0$, however, because in this case the slot is in the position of the shadow boundary at which the tangent plane approximation is known to be invalid.

It is found, from the work on high frequency diffraction by Fock,[3] that when $\theta_o = 0$ the component of the magnetic field along the slot is

$$\bar{H} \cdot \hat{\ell} \approx -\frac{1}{\sqrt{2}} \left\{ \begin{matrix} \cos \varphi_o \\ \sin \varphi_o \end{matrix} \right\} ,$$

for an incident field polarized in the $\left\{ \begin{matrix} x \\ y \end{matrix} \right\}$ direction. Therefore, when $\theta_o = 0$, (A.6) is replaced by

$$\left\{ \begin{matrix} \delta E_{xx} \\ \delta E_{yy} \\ \delta E_{xy} \end{matrix} \right\} = \frac{\alpha}{2} \int \left\{ \begin{matrix} \cos^2 \varphi_o \\ \sin^2 \varphi_o \\ \sin \varphi_o \cos \varphi_o \end{matrix} \right\} d\varphi_o \quad , \quad (\theta_o = 0) \quad ,$$

and the integration must now be carried out over the full length of the slot. This gives immediately $\delta E_{xy} \equiv 0$, as before, and

$$\delta E_{xx} = \delta E_{yy} \approx \alpha \frac{\pi}{2}, \quad (\theta_o = 0) \quad , \tag{A.9}$$

which is just half the result obtained by the formal substitution of $\theta_o = 0$ into (A. 6).

The total backscattered field is the sum of the field E_o scattered by the perfect sphere and the field δE radiated by the slot. The normalized back-scattering cross section σ is given therefore, to first order in δE, by

$$\sigma = \frac{|E_o + \delta E|^2}{|E_o|^2} = 1 + 2 \, \text{Re} \left\{ \frac{\delta E}{E_o} \right\} \quad,$$

where the Re stands for "real part of." Thus, from (A. 7), a radar sending and receiving signals polarized in the x direction measures a change $\delta\sigma_x$ in cross section of the sphere due to the slot given by

$$\delta\sigma_x(\theta_o) = \beta \, \frac{\cos(2ka \sin\theta_o + \psi_o)}{\sqrt{\sin\theta_o}} \tag{A. 10}$$

for θ_o bounded away from zero, and, from (A. 9),

$$|\delta\sigma_x(0)| \leq \frac{\beta}{2} \sqrt{\pi ka} \quad, \tag{A. 11}$$

where β and ψ_o are real constants. The unknown phase constant ψ_o in (A. 10) and the inequality in (A. 11) are necessary because the phase angle of the slot impedance is unknown.

For a y-polarized radar, the corresponding change $\delta\sigma_y$ in cross section is small compared with $\delta\sigma_x$ for θ_o bounded away from zero and $\delta\sigma_y(0) = \delta\sigma_x(0)$.

25

Since ka is large, the change in cross section when averaged over all aspect angles is essentially zero, due to the highly oscillatory nature of (A. 10). Thus the variance of the cross section is given directly by averaging the square of the change in cross section. For a radar polarized in the direction $\hat{x} \cos\varphi + \hat{y} \sin\varphi$, the change $\delta\sigma_\varphi(\theta_o)$ in cross section is clearly

$$\delta\sigma_\varphi(\theta_o) = \delta\sigma_x(\theta_o) \cos^2\varphi + \delta\sigma_y(\theta_o) \sin^2\varphi \tag{A. 12}$$

and the variance $\overline{[\delta\sigma_\varphi(\theta_o)]^2}$, averaged over all aspects and polarizations is,

$$\overline{[\delta\sigma_\varphi(\theta_o)]^2} = \frac{1}{2\pi} \int [\delta\sigma_\varphi(\theta_o)]^2 \sin\theta_o \, d\theta_o \, d\varphi \tag{A. 13}$$

where the limits for φ are $(0, 2\pi)$ and for θ_o are $(0, \pi/2)$, since the integrand is symmetrical in θ_o about the point $\theta_o = \pi/2$.

The result of combining (A. 12) and (A. 13) and carrying out the φ integration is

$$\overline{[\delta\sigma_\varphi(\theta_o)]^2} = \frac{1}{8} \int_0^{\frac{\pi}{2}} (3\delta\sigma_x^2 + 2\delta\sigma_x \delta\sigma_y + 3\delta\sigma_y^2) \sin\theta_o \, d\theta_o \quad .$$

Now both $\delta\sigma_x$ and $\delta\sigma_y$ are finite when $\theta_o = 0$ whereas $\sin\theta_o$ is zero. Also $\delta\sigma_y$ is essentially zero for θ_o bounded away from zero. Therefore only $\delta\sigma_x^2$ need be retained in the integrand so that, from (A. 10), the variance is given closely

by

$$\overline{[\delta\sigma_\varphi(\theta_o)]^2} = \frac{3}{8}\beta^2 \int\limits_o^{\frac{\pi}{2}} \cos^2(2ka\sin\theta_o + \psi_o)\,d\theta_o \quad .$$

But $2\cos^2(2ka\sin\theta_o + \psi_o) = 1 + \cos[2(2ka\sin\theta_o + \psi_o)]$ and since ka is large, the integral of the trigonometric term on the right in this expression is negligible compared with the integral of unity.

Thus the final expression for the variance is

$$\overline{[\delta\sigma_\varphi(\theta_o)]^2} = \frac{3\pi}{32}\beta^2 \quad . \tag{A.14}$$

A similar derivation for a circularly polarized radar leads to the result

$$\overline{[\delta\sigma_c(\theta_o)]^2} = \frac{\pi}{16}\beta^2 \quad . \tag{A.15}$$

27

REFERENCES

1. R. T. Prosser, "The Lincoln Calibration Sphere," Proc. IEEE (Correspondence), 53, 1672 (1965).

2. M. L. Burrows, "A Reformulated Boundary Perturbation Theory in Electromagnetism and its Application to a Sphere," (Submitted to the Physical Review).

3. V. A. Fock, Electromagnetic Diffraction and Propagation Problems, (Pergamon, New York, 1965), Chapter II.

4. J. Rheinstein, "Tables of the Amplitude and Phase of the Backscatter from a Conducting Sphere," Group Report 22G-16, Lincoln Laboratory, M. I. T. (June 1963).
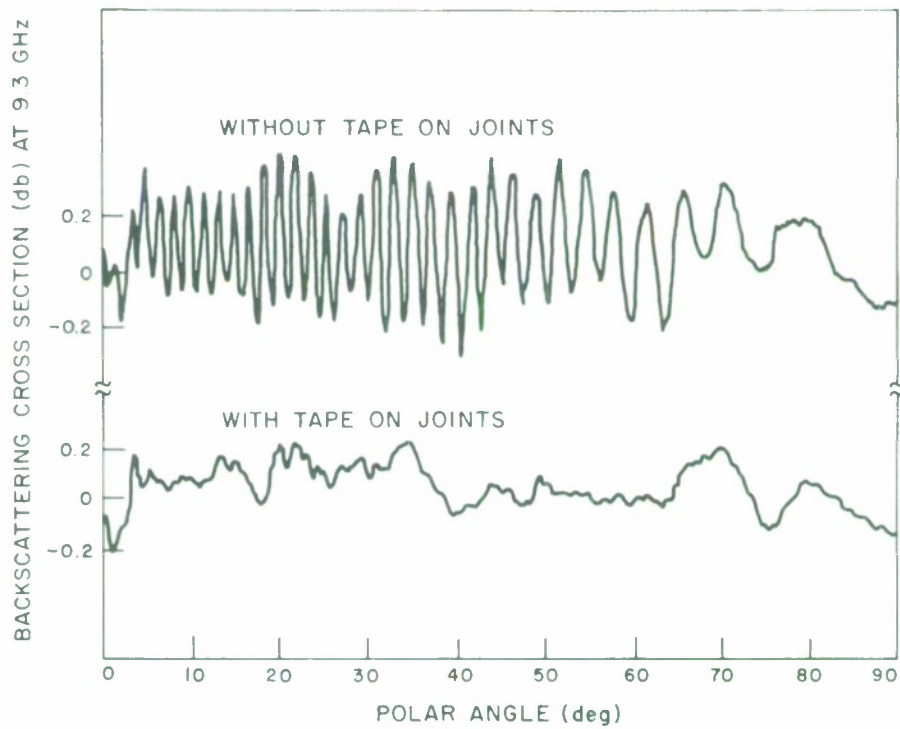
Fig. 1. Effect of unclosed butt joints on the backscattering cross section of the C sphere.
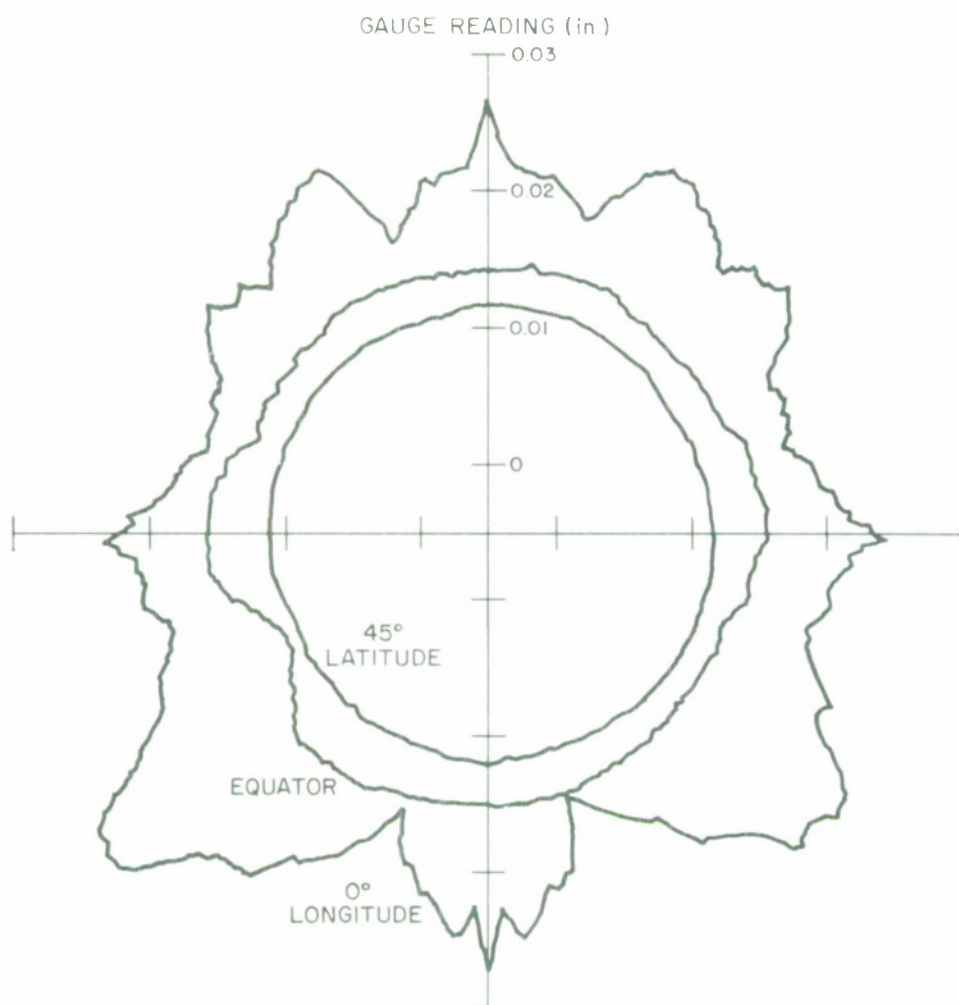
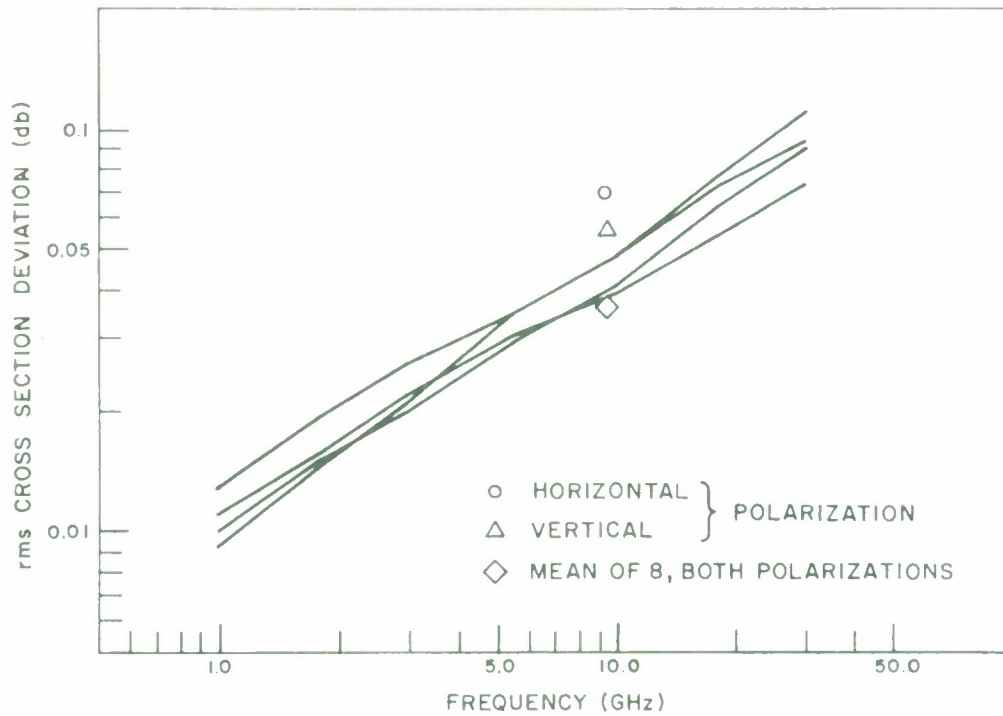Fig. 2. Dimensional profiles of the G sphere. The zero reference for each curve is chosen arbitrarily.
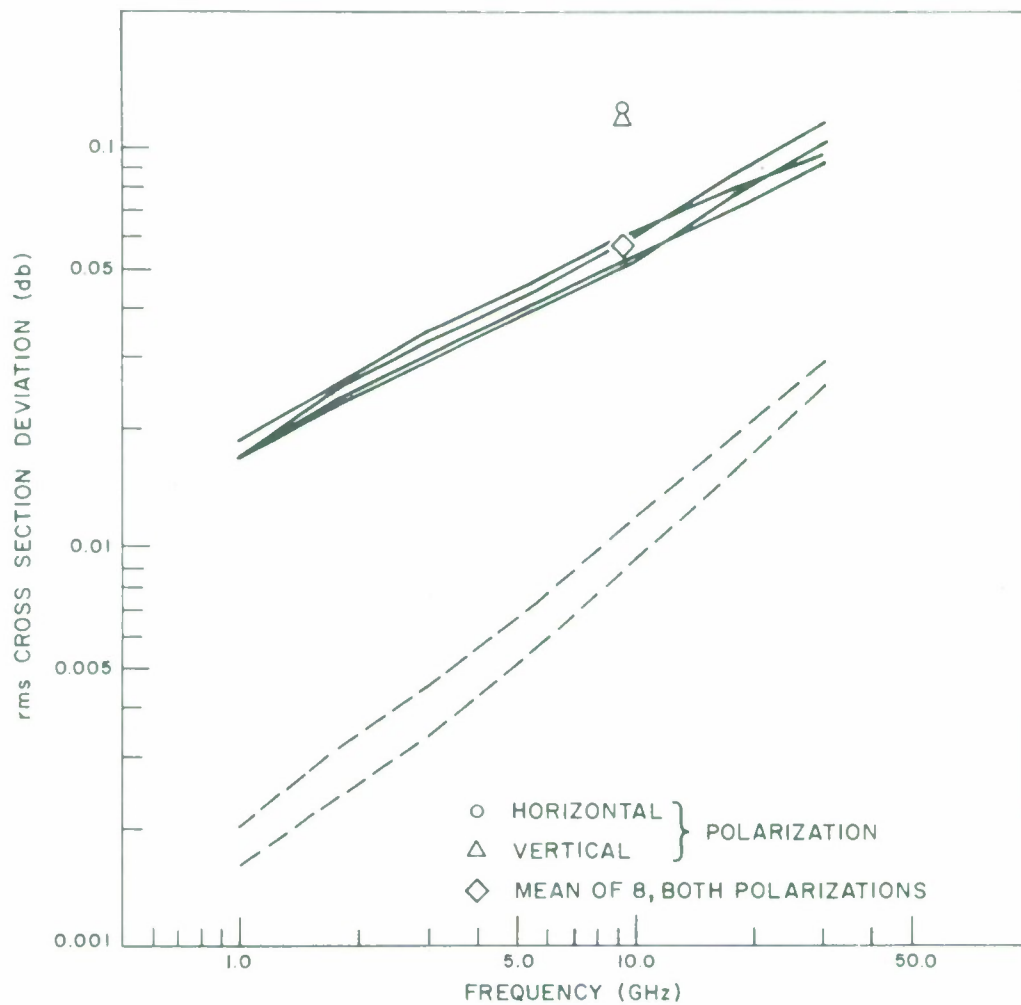
Fig. 3. Computed r. m. s. deviation of the backscattering cross
section of the G sphere as a function of frequency. The plotted
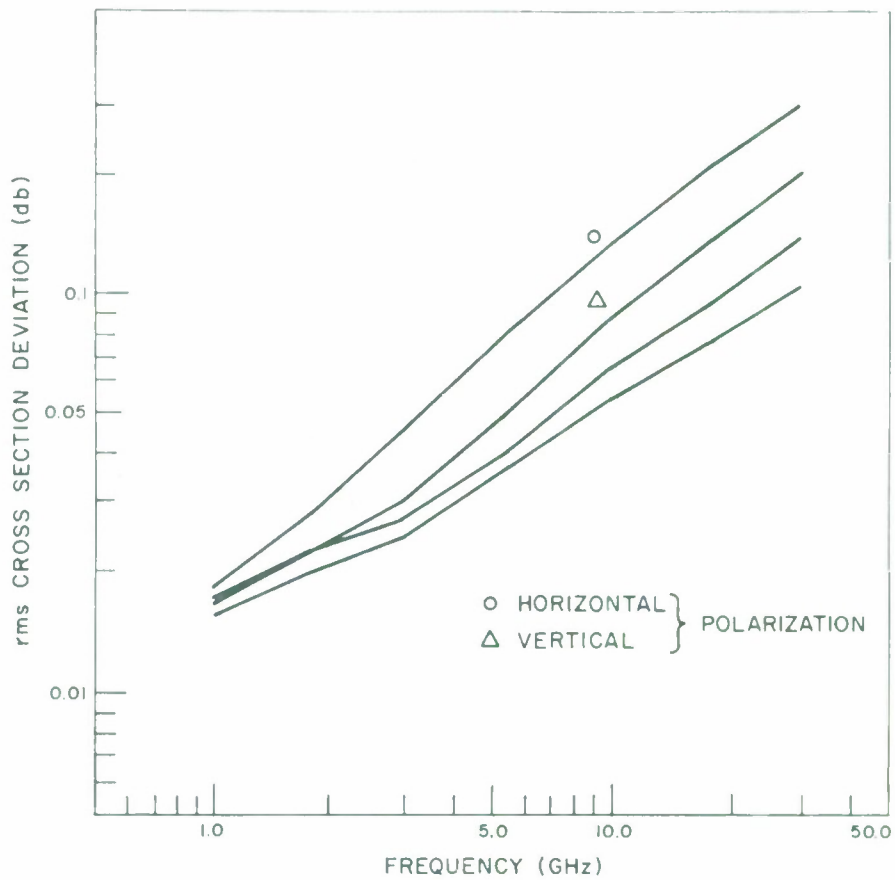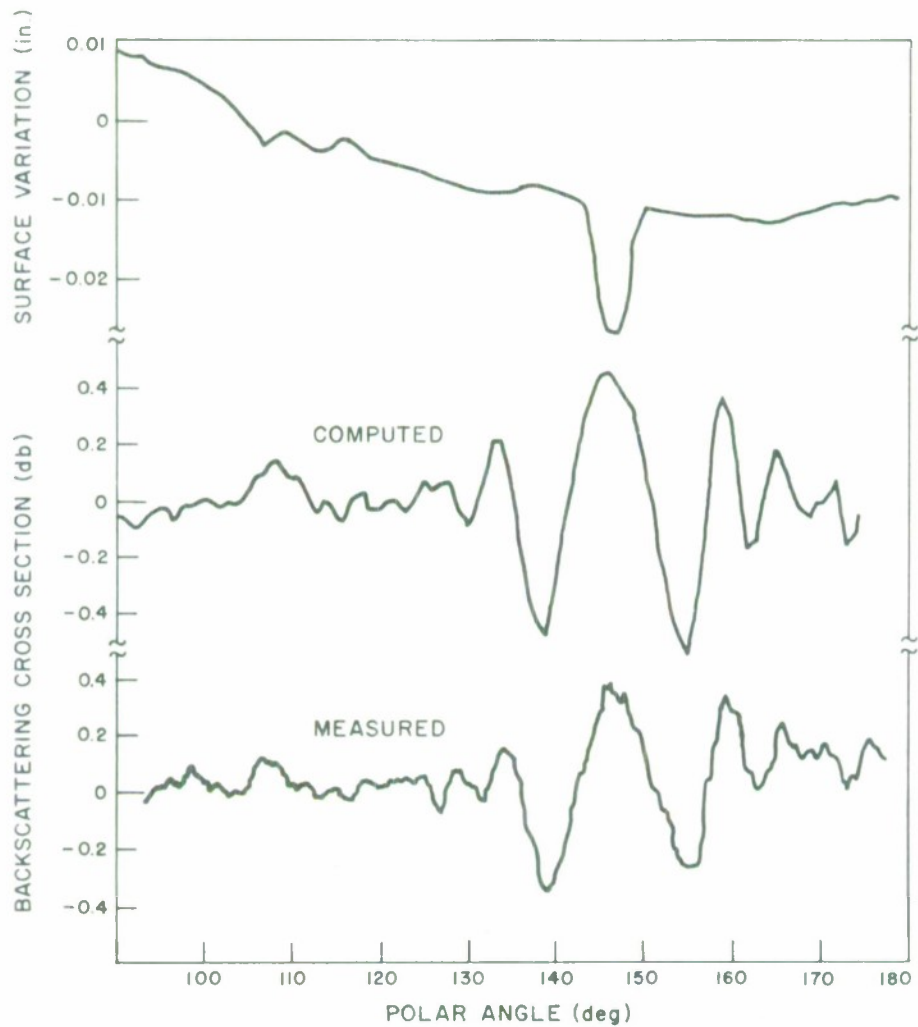points are based on range measurements.

Fig. 4. Computed r. m. s. deviation of the backscattering cross section of the F sphere as a function of frequency. The plotted points are based on range measurements.

Fig. 5. Computed r.m.s. deviation of the backscattering cross section of the C sphere as a function of frequency. The plotted points are based on range measurements.

Fig. 6. Sections from the polar profile, the calculated cross-
sectional variation and the measured cross-sectional variation
in the vicinity of the flat crescent on the C sphere. The cross
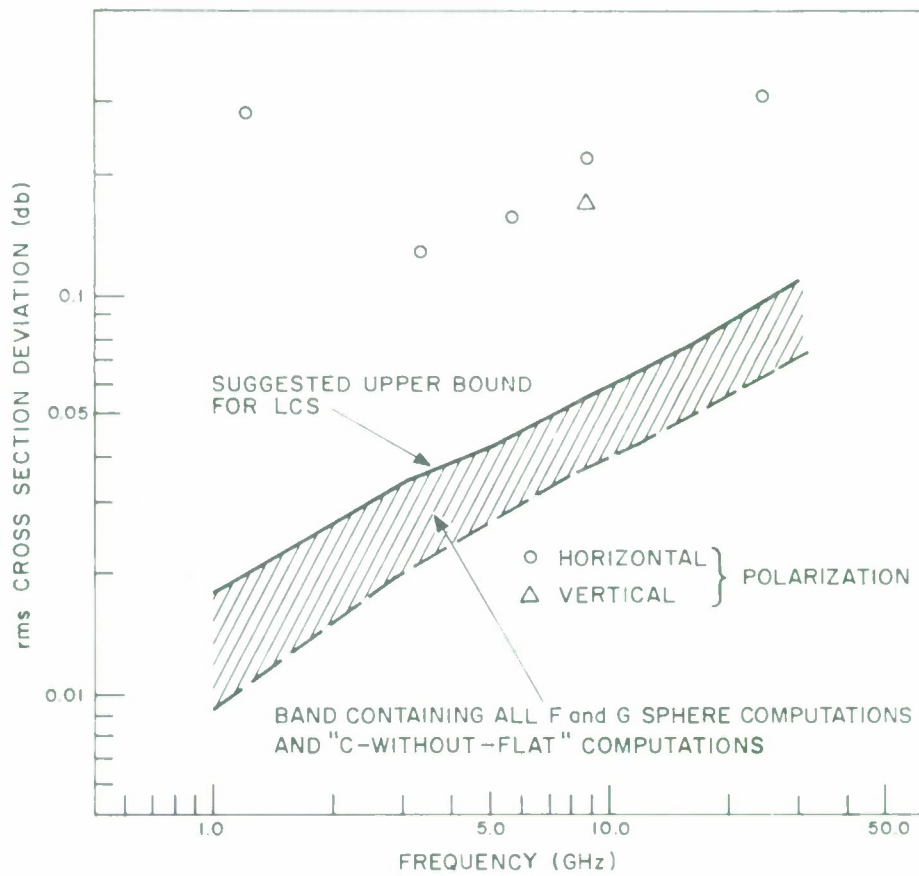sections were computed and measured at 9.3 GHz.

Fig. 7. The spread in radar quality of the F, G and "C-without-flat" spheres, the suggested upper bound on the quality of the LCS and the range measurements on the LCS.
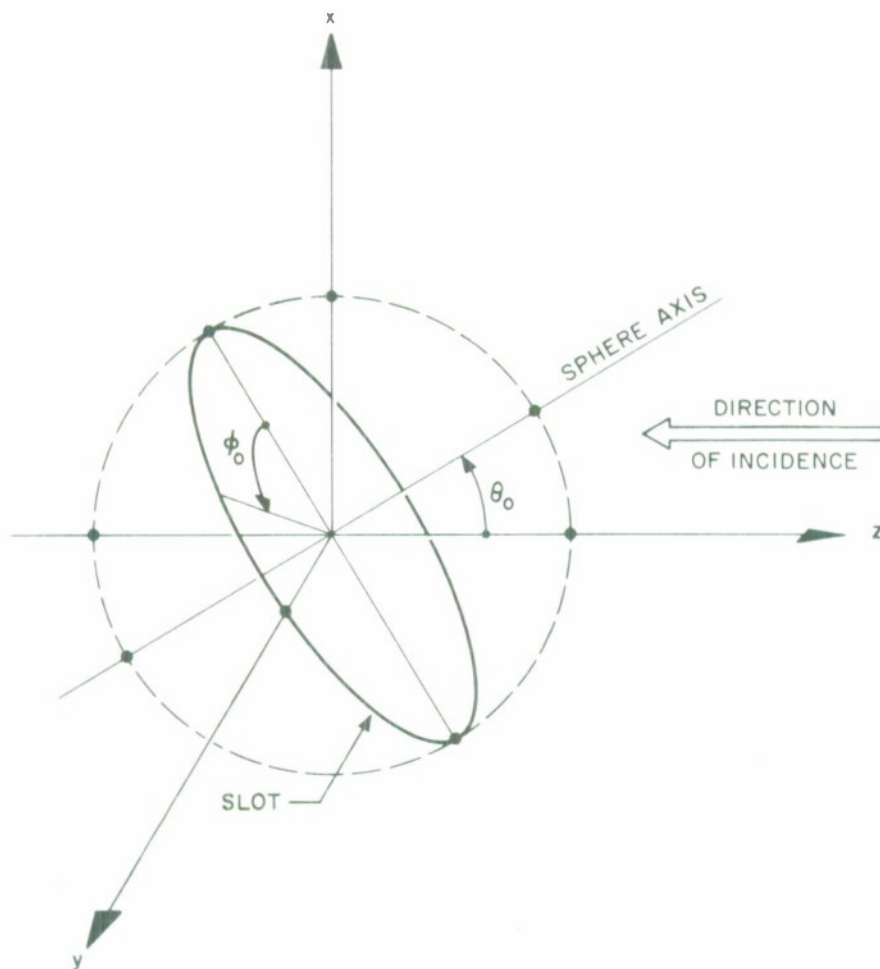
Fig. 8. Coordinate system for examining the field scattered by an equatorial slot.
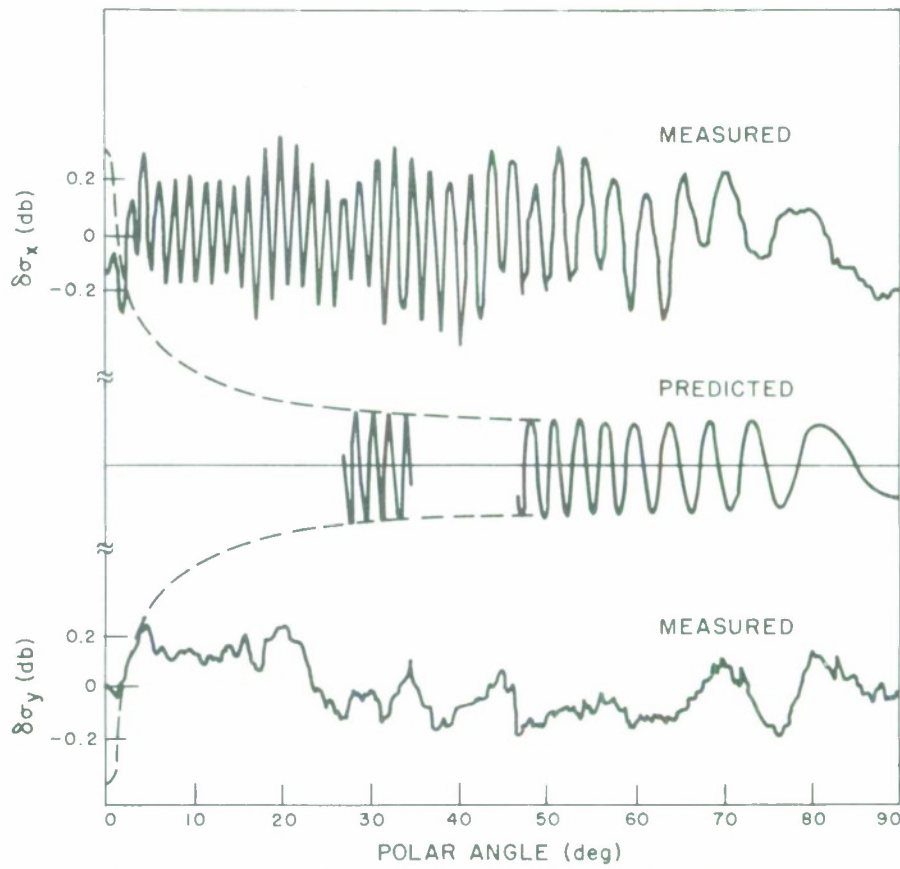
Fig. 9. Comparison of the measured and predicted effect of the butt joints on the sphere.
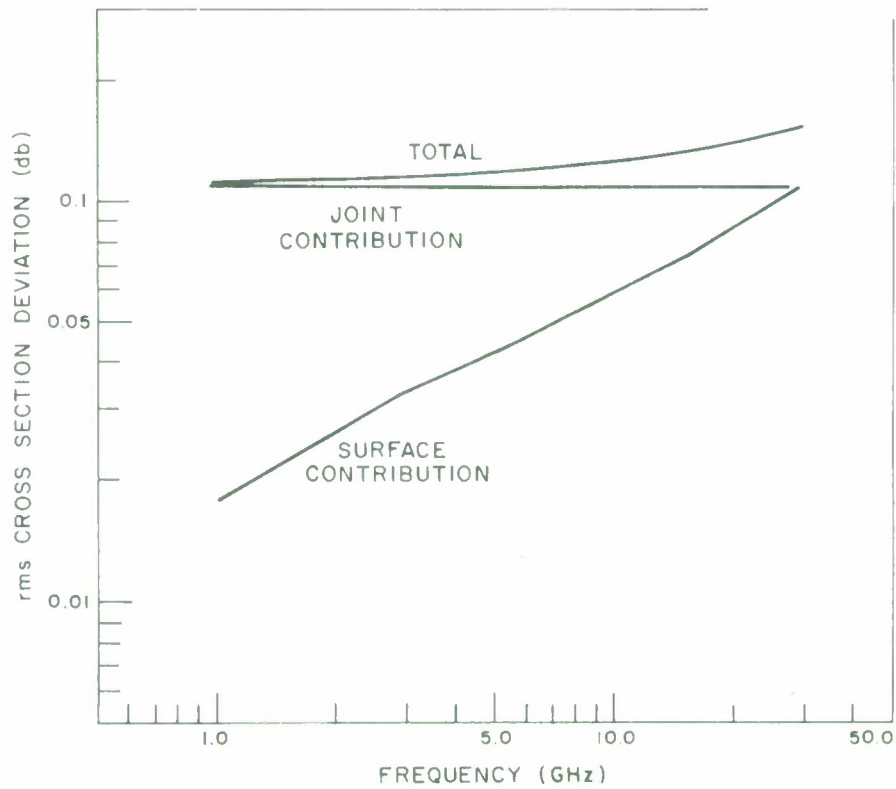
Fig. 10. Upper-bound estimates for the r.m.s. deviation of the total backscattering cross section of the LCS and for the r.m.s. deviations due to the surface perturbations and the joint separately.

DISTRIBUTION LIST

Division 6

    Dinneen, G. P.
    Morrow, W. E.
    Prosser, R. T.

Group 61

    Ricardi, L. J.
    Assaly, R. N.
    Burrows, M. L.
    Burns, R. J.
    Crane, R. K.
    Devane, M. E.
    Frediani, D. J.
    Lindberg, C. A.
    Niro, L.
    Rankin, J. B.
    Rosenthal, M. L.
    Sotiropoulos, A.
    White, S.

Group 62

    Lebow, I. L.
    Heart, F. E.
    Drouilhet, P. R.
    Nichols, B. E.

Group 63

    Sherman, H.
    Lerner, R. M.
    MacLellan, D. C.
    Waldron, P.
    Smith, W. B.
    Michelove, L. D.

Group 64

    Green, P. E.

Group 65

    Wood, R. V.

Group 66

    Reiffen, B.

Division 2

Group 22

    Rheinstein, J.

Division 3

    Chisholm, J. H.
    Ruze, J.

Group 31

    Sebring, P. B.
    Pettengill, G. H.
    Hagfors, T.
    Meeks, M. L.

Division 4

    Weiss, H. G.

Group 44

    Blake, C.

Group 45

Miller, S. J.

Group 46

Jones, C. W.
Keeping, K. J.

Division 7

Hutzenlaub, J. F.

Group 71

Blaisdell, E. W. (3)
DeSantis, F. G.

DOCUMENT CONTROL DATA – R&D

(Security classification of title, body of abstract and indexing annotation must be entered when the overall report is classified)

1. ORIGINATING ACTIVITY (Corporate author)	2a. REPORT SECURITY CLASSIFICATION
Lincoln Laboratory, M.I.T.	Unclassified
	2b. GROUP
	None

3. REPORT TITLE

The Quality of the Lincoln Calibration Sphere

4. DESCRIPTIVE NOTES *(Type of report and inclusive dates)*

Technical Note

5. AUTHOR(S) *(Last name, first name, initial)*

Burrows, Michael L.

6. REPORT DATE	7a. TOTAL NO. OF PAGES	7b. NO. OF REFS
22 August 1966	46	4

8a. CONTRACT OR GRANT NO.	9a. ORIGINATOR'S REPORT NUMBER(S)
AF 19(628)-5167	
b. PROJECT NO.	Technical Note 1966-41
Order 600	
c.	9b. OTHER REPORT NO(S) *(Any other numbers that may be assigned this report)*
d.	ESD-TR-66-417

10. AVAILABILITY/LIMITATION NOTICES

Distribution of this document is unlimited.

11. SUPPLEMENTARY NOTES	12. SPONSORING MILITARY ACTIVITY
None	Advanced Research Projects Agency Department of Defense

13. ABSTRACT

Due to the relatively high background noise level of the radar range used to measure the Lincoln Calibration Sphere (LCS) before launch, the upperbound estimates of the backscattering cross section variation made at the time included a large contribution generated by the range itself. By comparing the range measurements and the mechanical measurements made on the LCS with measurements made on three other similarly constructed spheres, a refined estimate of the quality of the LCS is made. The comparison makes use of more precise range and mechanical measurements made on the other three spheres and of an application of perturbation theory to compute the variation of cross section from the mechanical measurements. The unexpectedly large signal scattered by the equatorial joint is an unwelcome addition to the backscattered field and is discussed in some detail.

It is concluded that, at all frequencies below about 25 GHz, the r.m.s. deviation in backscattering cross section is not greater than 0.15 db, and that the average backscattering cross section differs from that of a perfect sphere of radius 0.56469 m by an amount which is small compared with the r.m.s. deviation.

14. KEY WORDS

Lincoln Calibration Sphere
backscattering cross section
radar calibration target
perturbation theory